HIGHER-RESOLUTION DETERMINATION OF ZERO-OFFSET COMMON-REFECTION-SURFACE (CRS) STACK PARAMETERS

E.G. Asgedom, M. Tygel, and L.-J. Gelius

email: *mtygel@gmail.com*
keywords: *CRS, MUSIC, semblance, covariance*

ABSTRACT

In this paper we developed a higher resolution method for the estimation of the three traveltime parameters that are used in the 2D zero-offset, Common-Reflection-Surface stack method. The underlying principle in this method is to replace the coherency measures performed using semblance with that of MUSIC (MUltiple SIgnal Classification) pseudo-spectrum that utilizes the eigenstructure of the data covariance matrix. The performance of the two parameter estimation techniques (i.e. semblance and MUSIC) was investigated using synthetic seismic diffraction and reflection data corrupted with white Gaussian noise. The estimated parameters employing MUSIC were shown to be superior of those from semblance.

INTRODUCTION

Many important tasks in seismic processing and imaging require the estimation of traveltime parameters. Such parameters include, among others, *velocities* (e.g., for stacking and time-migration purposes), traveltime slopes and curvatures (e.g., for slant, common-reflection-surface (CRS), multifocus (MF) stacks) and event picking for tomographical methods. As shared with many other areas of activity, a basic feature of seismic signals (referred to as *events*) is that they exhibit some sort of *coherent* or *aligned* energy. More specifically, seismic events (e.g., reflections or diffractions) align themselves along curves or surfaces (referred to as *moveouts*) within the data. The basic strategy for signal detection and information extraction, is to express these moveouts as a function of a few, meaningful parameters, and to estimate such parameters so as the moveout optimally approximates the events. In general, the search for parameters, sometimes referred to as *wavefront shaping parameters*, carry key information about the geological structure under investigation.

To assess how well a moveout, defined by some trial parameters, approximates a target signal, a number of quantifiers (or *coherence measures*) has been proposed. General discussions on coherency measures applied to seismic data can be found in the pioneering papers of Taner and Koehler (1969), Neidell and Taner (1971), Gelchinsky et al. (1985), with a clear emphasis on the second-order coherence measure *semblance*. Semblance quantify the likelihood between the trial moveout and the target event by stacking the data along that moveout and measuring the energy of the output.

Adopting the notation as in Kirlin (1992), for a given sample, k, at a given (reference) trace, the so-

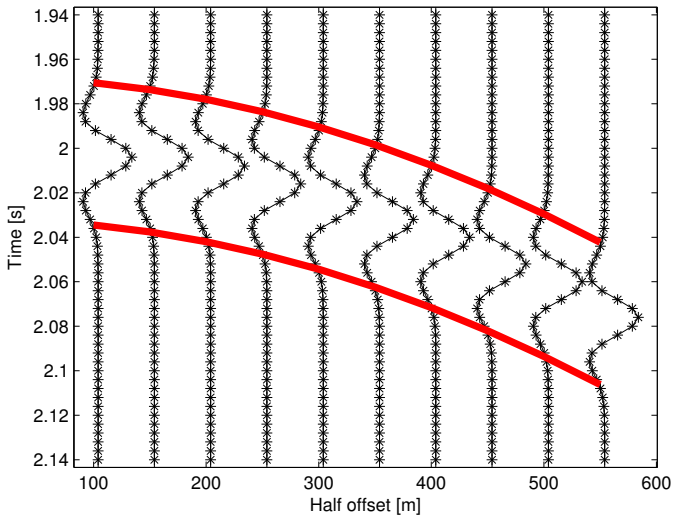

Figure 1: Time window used to compute semblance.The two red lines show the traveltime trajectories bounding the window used to select the data.

called *semblance coefficient*, or simply *semblance*, S_c, can be mathematically written in the form

$$S_c = \frac{\sum_{j=k-N/2}^{j=k+N/2} \left| \sum_{i=1}^{M} x(j,i) \right|^2}{M \sum_{j=k-N/2}^{j=k+N/2} \sum_{i=1}^{M} |x(j,i)|^2} \,. \tag{1}$$

Here the semblance coefficient is computed for N samples taken from M traces in a window centered about the trajectory defined by the moveout equation generated by the trial traveltime parameters (cf. Figure 1). In the following, the given sample, k, and reference trace, as well as the number of samples, N, and number of traces, M, will be fixed throughout. As a consequence, we do not need to incorporate them into the semblance notation, which will be simply written as S_c. To construct the window in Figure 1, proper interpolation is performed to select the appropriate samples. In the language of electrical engineers, the above-described windowing process *steers* the stacking along the trial moveout.

Semblance can be described in terms of the covariance matrix, of the data. Following, e.g., Du and Kirlin (1993), within the selected time window along the chosen trial moveout, semblance can be written in the form

$$S_c = \frac{\mathbf{u}^T \mathbf{R} \mathbf{u}}{M tr(\mathbf{R})} \,, \tag{2}$$

where $\mathbf{u}$ is a column vector of ones, which can be referred to as the *unitary steering* vector, and $\mathbf{R}$ is the covariance of the data. Assuming the different sources can be described by a zero-mean stochastic process, the data covariance matrix is given as

$$\mathbf{R} = E\{\mathbf{D}\mathbf{D}^H\} \,, \tag{3}$$

where $\mathbf{D} = (d_{ij})$ is the data matrix, in which d_{ij} is the recorded data at the i-th trace and j-th sample. As in usual notation, $E\{\}$ and $tr()$ represent the expected value and matrix trace, respectively. Moreover, superscripts T and H represent transpose and conjugate transpose, respectively. As pointed out by Neidell and Taner (1971), equation 2 provides the interpretation that semblance can be regarded, within the selected time window, as a normalized output/input energy ratio. The denominator, $tr(\mathbf{R})$, is the normalization used by semblance in order to generate a maximum peak of unity at the "correct" moveout parameters (namely, the ones for which we have the optimal stack).

Even though semblance is a good measure of coherency, it can in many times provide insufficient resolution for the parameter estimation. That is the case, in particular, for interfering events. There is, thus, a motivation to look for alternatives to overcome these difficulties. As recognized in sonar and radar applications, methods exploiting the properties of the eigenstructure (namely, eigenvalues and eigenvectors) of the data covariance matrix can lead to far better resolution results than semblance (Schmidt, 1986; Biondi and Kostov, 1989; Kirlin, 1992).

The basic idea of the eigenstructure approach is to decompose the data covariance matrix into two orthogonal subspaces. The first is the *signal* subspace, which is generated by the eigenvectors associated to high eigenvalues. The second is the *noise* subspace, generated by the small or zero eigenvalues. In this paper, we use the eigenstructure method called *MUltiple SIgnal Classification (MUSIC)*, introduced by Schmidt (1986). MUSIC exploits the fact that the "correct" moveout, represented as a steering vector, must lie in the signal subspace and therefore is orthogonal to the noise subspace eigenvectors. As a consequence, the *projection* of the steering vector onto the noise subspace provides a nearly vanishing value. The inverse of such a projection (namely the sum of the dot products of the steering vector with the noise eigenvectors) should peak when the steering vector represents a correct moveout.

This work can be seen as a follow up of Biondi and Kostov (1989), in which the application of MUSIC to single-parameter velocity analysis and slant stacks is described. Here, we extend the application of MUSIC to Common-Reflection-Surface (CRS) multi-parameter estimation. Besides the theoretical exposition of the technique, applications to first synthetic examples, consisting of dipping planar reflectors and point diffractors, are provided. Comparisons of the obtained results and conventional semblance confirm, at least for these initial examples, the expected far better resolution of MUSIC.

CLASSICAL MUSIC: NARROWBAND AND UNCORRELATED SIGNALS

In its original or classical form (Schmidt, 1986), MUSIC considers an array of N_r receivers recording W incoming reflected or diffracted signals, in an arbitrary background medium. In time domain, the data recorded by the i-th receiver can be modeled as

$$d_i(t) = \sum_{\mathsf{w}=1}^{W} s_{\mathsf{w}}(t - \tau^{\theta}_{i,\mathsf{w}}) + n_i(t) \;, \quad (i = 1, 2, \ldots, N_r) \;, \tag{4}$$

where $s_{\mathsf{w}}(t)$ is the source pulse associated with event w, and $n_i(t)$ is the additive random noise at the i-th receiver. Finally, $\tau^{\theta}_{i,\mathsf{w}}$ is the traveltime (or time delay) of the w-th incoming signal (or event) arriving at the i-th receiver. The superscrit, θ, indicates that the moveouts depend on a set of one or more parameters, here denoted, by a so-called *parameter vector*, $\boldsymbol{\theta}$. The most popular trial-moveout example is the normal-moveout (NMO), applied for velocity analysis in the common-midpoint (CMP) configuration. In the 2D situation, the single parameter to be estimated is the NMO-velocity. An example of multi-parameter moveout is the general hyperbolic moveout used by the common-reflection-surface (CRS) stacking method. As previously indicated, application of MUSIC to velocity analysis has been described by Biondi and Kostov (1989). Here we extend the analysis to CRS parameter estimation in 2D data. In this situation, three parameters are to be estimated. In order not to disturb the main flow, the description of the generalized hyperbolic or, more simply, the CRS traveltimes, $\tau_{i,\mathsf{w}}$, are postponed to Appendix A.

Narrowband signals

For narrowband signals $s_{\mathsf{w}}(t)$ the traveltimes can be expressed as exponential phase shifts around the center angular frequency ω. For notation simplicity, that fixed frequency will be omitted. As a consequence, the data model in equation (4) can be recast as

$$d_i(t) = \sum_{\mathsf{w}=1}^{W} s_{\mathsf{w}}(t) \exp\left(-i\omega\tau^{\theta}_{i,\mathsf{w}}\right) + n_i(t) \;. \tag{5}$$

After time discretization, the above equation can be recast in matrix form as

$$\mathbf{D} = \mathbf{A}(\boldsymbol{\theta})\mathbf{S} + \mathbf{N} \;, \tag{6}$$

where $\mathbf{D} = (d_{ij}) = (d_i(t_j))$ and $\mathbf{N} = (n_{ij}) = (n_i(t_j))$ are, respectively, the $N_r \times N_t$ *data* and *additive noise* matrices, and $\mathbf{S} = (s_{\mathsf{w}j}) = (s_{\mathsf{w}}(t_j))$ is the $W \times N_t$ *source* matrix. Finally,

$$\mathbf{A}(\boldsymbol{\theta}) = (\mathbf{a}_1(\boldsymbol{\theta}), \ldots, \mathbf{a}_{\mathsf{w}}(\boldsymbol{\theta}), \ldots, \mathbf{a}_W(\boldsymbol{\theta})) \tag{7}$$

is the $N_r \times W$ *array response matrix* containing all the *steering vectors*

$$\mathbf{a}_{\mathsf{w}}(\boldsymbol{\theta}) = \begin{bmatrix} \exp(-i\omega\tau^{\theta}_{1,\mathsf{w}}) \\ \exp(-i\omega\tau^{\theta}_{2,\mathsf{w}}) \\ \cdot \\ \cdot \\ \cdot \\ \exp(-i\omega\tau^{\theta}_{N_r,\mathsf{w}}) \end{bmatrix} . \tag{8}$$

MUSIC utilizes the eigenstructure of the data covariance matrix defined by equation 3. Substituting equation (6) into equation (3) and assuming uncorrelated noise with variance of σ_n^2, the covariance matrix can be recast as

$$\mathbf{R} = \mathbf{A}(\boldsymbol{\theta})[E\{\mathbf{S}\mathbf{S}^H\}]\mathbf{A}(\boldsymbol{\theta})^H + E\{\mathbf{N}\mathbf{N}^H\} = \mathbf{A}(\boldsymbol{\theta})\mathbf{R}_s\mathbf{A}(\boldsymbol{\theta})^H + \sigma_n^2\mathbf{I} \, , \tag{9}$$

where $\mathbf{R}_s$ and $\mathbf{I}$ are respectively the source covariance and identity matrices. The MUSIC algorithm performs an eigendecomposition of this covariance matrix

$$\mathbf{R}\mathbf{U} = \boldsymbol{\Lambda}\mathbf{U} \, , \tag{10}$$

where $\boldsymbol{\Lambda}$ =diag$(\lambda_1, \lambda_2, \ldots, \lambda_{N_r})$ contains the eigenvalues satisfying $\lambda_1 \geq \lambda_2 \geq \cdots \geq \lambda_{N_r}$, and $\mathbf{U} = [\mathbf{u}_1, \mathbf{u}_2, \ldots, \mathbf{u}_{N_r}]$ are the corresponding orthonormal eigenvectors of $\mathbf{R}$. The unitary matrix of eigenvectors $\mathbf{U}$ can be decomposed further as $\mathbf{U} = [\mathbf{U}_s \ \mathbf{U}_n]$, where the columns of $\mathbf{U}_s$ comprise the eigenvectors corresponding to the largest eigenvalues of $\mathbf{R}$ (the signal subspace), and with $\mathbf{U}_n$ containing the remaining (noise) eigenvectors.

Uncorrelated signals

For MUSIC to be applicable in our parameter search problem, the different source pulses, $s_{\mathsf{w}}(t)$, should be uncorrelated resulting in a covariance matrix $\mathbf{R}_s$ having full rank equal to the number of events W recorded at the receivers. If the M source vectors are linearly independent then the matrix $\mathbf{R}_s$ is positive-definite which results in $\mathbf{A}(\boldsymbol{\theta})\mathbf{R}_s\mathbf{A}(\boldsymbol{\theta})^H$ to be a positive semi definite matrix with its rank spanning the steering vectors corresponding to the appropriate parameters we are searching. With the above condition satisfied and since the noise subspace is orthogonal to the signal subspace, the MUSIC *pseudo-spectrum*, $\mathbf{P}_{MU}(\boldsymbol{\theta})$, is given by

$$\mathbf{P}_{MU}(\boldsymbol{\theta}) = \frac{\mathbf{a}(\boldsymbol{\theta})\mathbf{a}(\boldsymbol{\theta})^H}{\mathbf{a}(\boldsymbol{\theta})\mathbf{P}_n\mathbf{a}(\boldsymbol{\theta})^H} \, , \tag{11}$$

where $\mathbf{a}(\boldsymbol{\theta})$ is the test steering vector and $\mathbf{P}_n$ is the noise subspace projection matrix given by $\mathbf{P}_n = \mathbf{U}_n\mathbf{U}_n^H$. Since the steering vectors $\mathbf{a}(\boldsymbol{\theta})$ are orthogonal to the eigenvectors spanning the noise subspace $\mathbf{u}_n$, it follows that the parameter estimates will occur at those parameter values for which we have

$$\mathbf{a}(\boldsymbol{\theta})\mathbf{P}_n\mathbf{a}(\boldsymbol{\theta})^H \approx 0 \, . \tag{12}$$

This corresponds to large peaks in the MUSIC pseudo-spectrum as given by equation (11).

Wideband uncorrelated signals

As indicated above, the MUSIC algorithm was originally developed for narrowband and uncorrelated signal applications. If the condition of uncorrelated signals is maintained, an alternative to this situation is to decompose a wideband data into narrowband data components and then treat each narrowband separately

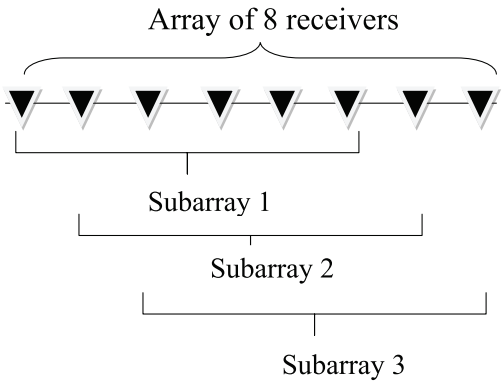

Figure 2: Concept of spatial smoothing.

(Biondi and Kostov, 1989). The MUSIC pseudo-spectrum at the center angular frequency ω_i of the i-th narrowband now takes the form

$$\mathbf{P}_{MU}(\boldsymbol{\theta};\omega_i) = \frac{\mathbf{a}(\boldsymbol{\theta};\omega_i)\mathbf{a}(\boldsymbol{\theta};\omega_i)^H}{\mathbf{a}(\boldsymbol{\theta};\omega_i)\mathbf{P}_n(\omega_i)\mathbf{a}(\boldsymbol{\theta};\omega_i)^H} \ , \tag{13}$$

where $\mathbf{a}(\boldsymbol{\theta};\omega_i)$ and $\mathbf{P}_n(\omega_i)$ are respectively the test steering vector and the noise subspace projection matrix at the the i-th center angular frequency ω_i. The strategy followed in this work is to Fourier transform the test data and select a narrowband close to the center frequency of the source pulse as input to MUSIC.

SEISMIC MUSIC: WIDEBAND AND CORRELATED SIGNALS

Seismic signals are highly correlated and require a special modification to be used by the original MUSIC algorithm. The consequence of having correlated sources is that there will be a rank deficiency in the source covariance matrix $\mathbf{R}_s$ that will result in a mix of signal and noise subspaces. As a result, the MUSIC algorithm will loose its power to peak at the appropriate estimated parameters.

In order to handle correlated sources, spatial smoothing over the covariance matrix, can be employed (Biondi and Kostov, 1989). The idea is to subdivide the array of N_r sensors into K identical overlapping subarrays of $N_r - K + 1$ receivers (cf. Fig 2) and then compute the covariance for all the subarrays and average the result. If the covariance matrix for subarray k is $\mathbf{R}_k$, the spatially smoothed covariance is given by

$$\mathbf{R}_K = \frac{1}{K}\sum_{k=1}^{K}\mathbf{R}_k \ . \tag{14}$$

To be able to implement spatial smoothing within seismics, one has to taper the data within a window following the event(s) (cf. Figure 1). The purpose of this tapering is to make the delay times of the event linear (which is the basic requirement behind spatial smoothing) (Biondi and Kostov, 1989).

The other advantage of performing the analysis in a given window is to make the steering vectors, required for generating the MUSIC pseudo-spectrum, to be frequency independent. This allows us to handle wideband seismic data. This process of windowing the event can also be interpreted as steering of the correlation matrix before eigendecomposition and using unity steering vectors for generating the MUSIC pseudo-spectrum (Kirlin, 1992).

Ideally, when the window is "perfectly" matching the event, which will be the case of an optimal choice of the moveout parameters, the signal would be flattened and all traces will nearly have the same moveout. As a consequence, the steering vectors used in equation (11) will be simply replaced by a vector of ones

making them frequency independent. In this situation, the MUSIC pseudo-spectrum generates a peak resulting in the identification of the correct estimates of the parameters.

In practice, the windows are constructed by moveouts, defined by trial parameters. Peaking of the corresponding MUSIC pseudo-spectra identifies, thus, the correct parameters. Following this approach, Kirlin (1992) has shown that MUSIC can be applied for the single-parameter case of velocity analysis. In other words, the objective was to obtain a high-resolution velocity spectrum. In this work, we extend that strategy to the CRS muti-parameter estimating problem. In other words, our objective is to obtain high-resolution estimates of the CRS parameters, which are three in the present 2D situation.

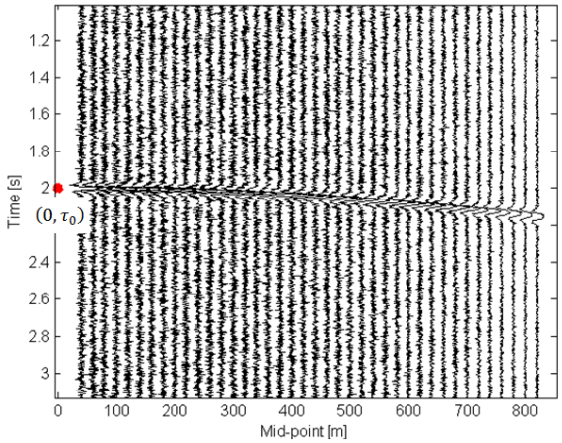

Figure 3: Synthetic CMP data used for comparison of MUSIC with semblance. A point diffractor and a dipping reflector ($\beta = 20^0$) with the same $\tau_0 = 2sec.$ is used to generate the data. Note that the two events are very close to each other and it is difficult to distingush them.

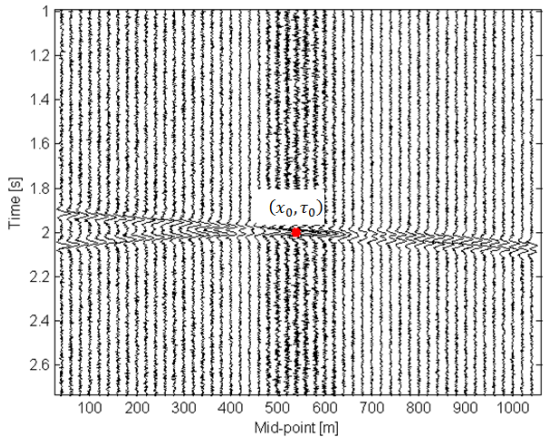

Figure 4: Synthetic ZO section used for comparison of MUSIC with Semblance. A point diffractor and a dipping reflector ($\beta = 20^0$) is used to generate the data. The red dot ($x_0 = 540m$ and $\tau_0 = 2sec.$) shows the location where we performed the parameter search.

NUMERICAL EXAMPLES

In this section we compare MUSIC and semblance for traveltime parameter estimation in the situations of classical MUSIC (narrowband uncorrelated signals) and seismic MUSIC (wideband correlated signals). For a simple model of a point diffractor and a dipping reflector with a homogeneous overburden, we analysed the cases: (a) CMP configuration, which requires the determination of a single parameter, C of

CRS traveltime (cf. A-1) and (b) ZO configuration, which requires the determination of two parameters, namely parameters A and B of the CRS traveltime (cf. A-1). The two events (diffraction and reflection) were chosen to be almost undistinguishable. All the test parameter points within RMS velocities of [1000:7.5:4000] m/s were tested for parameter C and $[-4\times10^{-}4{:}1\times10^{-}5{:}4\times10^{-}4]$ for parameter A and $[-3\times10-6{:}1\times10-7{:}3\times10-6]$ for parameter B. As seen below, in all situations, MUSIC performed much better then semblance.

Classical MUSIC

To illustrate the application of MUSIC for narrowband uncorrelated signals we considered a point diffractor and a dipping reflector illuminated under a CMP configuration. For a given CMP gather, the data consists of (compare with equation 5)

$$d_i(t) = s_{diff}(t)\exp(-i\omega\tau_{diff}) + s_{dip}(t)\exp(-i\omega\tau_{dip}) + n_i(t)\ , \tag{15}$$

where s_{diff} and s_{dip} are the sources and τ_{diff} and τ_{dip} are the traveltimes for the diffractor and dipping reflector events, respectively. Moreover, $n_i(t)$ is the additive noise. The traveltimes for these two events are described by the ordinary NMO equations

$$\tau^2_{diff}(h) = T_0^2 + C_{diff}h^2 \quad \text{and} \quad \tau^2_{dip}(h) = T_0^2 + C_{dip}h^2\ , \tag{16}$$

where the velocity coefficients for the diffractor, C_{diff}, and dipping reflector, C_{dip}, are given by

$$C_{diff} = \frac{4}{v^2_{RMS}} \quad \text{and} \quad C_{dip} = \frac{4\cos^2\beta}{v_{RMS}}\ . \tag{17}$$

Here, v_{RMS} and β represent the root mean square (RMS) velocity and the dip angle, respectively.

The sources, $s_{diff}(t)$ and $s_{dip}(t)$ are produced by a single narrowband source, $s(t)$, modified by two realizations of a random phase perturbations, $\phi_{diff}(\omega)$ and $\phi_{dip}(\omega)$, so as to produce uncorrelated sources. In frequency domain, this process is generally described as

$$s_{diff}(\omega) = s(\omega)\exp[i\phi_{diff}(\omega)] \quad \text{and} \quad s_{dip}(\omega) = s(\omega)\exp[i\phi_{dip}(\omega)]\ . \tag{18}$$

A synthetic CMP gather was generated employing equations (16) and (18) together with a Ricker zero-phase wavelet with a center frequency of 20 Hz (cf. Fig. 3). The fold was 40 representing a half-offset range from 40 m to 820 m. The data was sampled with 2 ms and white Gaussian noise with a variance of 10% of the maximum trace amplitude was added. The parameter estimation process was benchmarked using the classical semblance analysis of Neidell and Taner (1971).

The output from MUSIC (cf. equation (13)) is shown in Figure 5 together with the result obtained using semblance. As a result, MUSIC is seen to outperform semblance and resolve the two parameters well.

To perform a two-parameter test, we have now simulated a zero-offset (ZO) section for the same previous point diffractor and dipping reflector (cf. Fig. 4). The corresponding two ZO traveltimes for diffraction and reflection now are given by

$$\tau^2_{diff}(x_m) = \tau_0^2 + B_{diff}(x_m - x_0)^2 \quad \text{and} \quad \tau^2_{dip}(x_m) = [\tau_0 + A_{dip}(x_m - x_0)]^2\ , \tag{19}$$

with $B_{diff} = C_{diff}$ and $A_{dip} = 1.71\times10^{-4}$ (corresponding to a dip of 20^0 and a homogeneous medium with constant velocity 2000 m/s). As seen from Appendix A, the above equations represent the generalized hyperbolic (CRS) traveltime of equation A-1, in which the conditions

$$B_{diff} = C_{diff} \quad \text{and} \quad B_{dip} = 0\ , \tag{20}$$

have been implemented. As indicated in Appendix A, the far left equation above represents the diffraction condition. The far right equation is due to the fact that, in this considered experiment, the N-wave is planar.

Based on equations (19), using the previous uncorrelated sources (18), synthetic ZO data were computed for midpoints between 40m and 1040m. The results from the two-parameter search (A and B) are shown for respectively MUSIC (cf. Figure 6) and semblance (cf. Figure 7). MUSIC gives well resolved results as opposed to the semblance where the estimated parameters are more inaccurate.

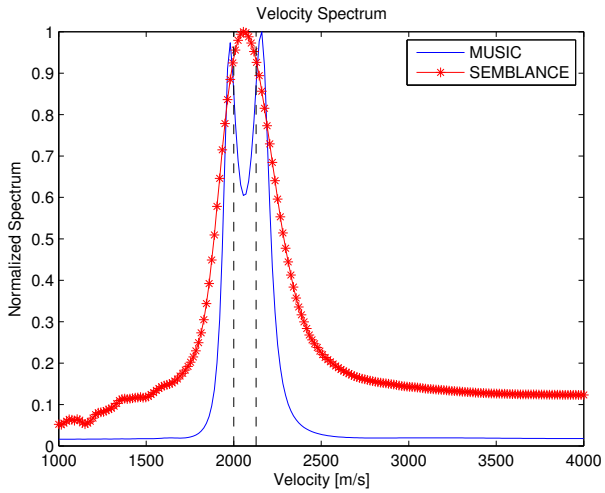

Figure 5: Spectrum of parameter C using both MUSIC and semblance (point diffractor and a dipping reflector $\beta = 20^0$). The black dotted lines show the correct location of the parameters C_{diff} and C_{dip}. We see that only MUSIC was able to resolve the two parameters.

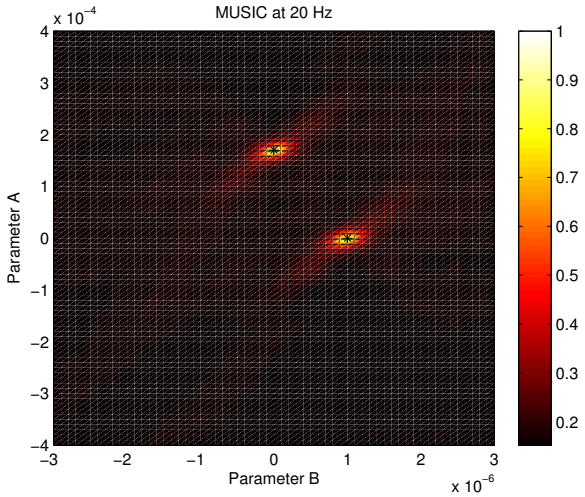

Figure 6: Determination of parameters A and B based on MUSIC for a diffractor and a dipping reflector $\beta = 20^0$. The black stars show the correct parameter locations.

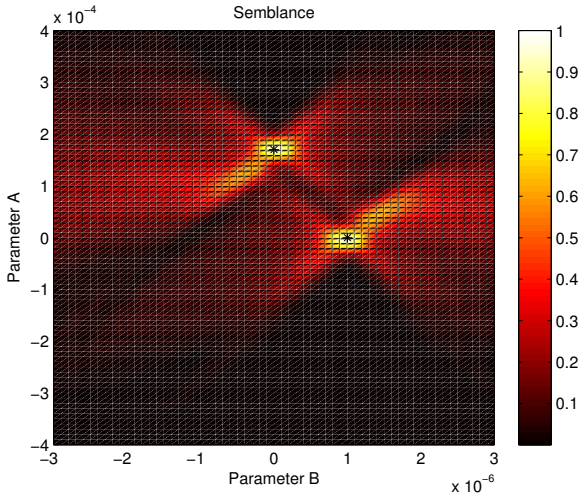

Figure 7: Determination of parameters A and B based on semblance for a diffractor and a dipping reflector $\beta = 20^0$. The black stars show the correct parameter locations.

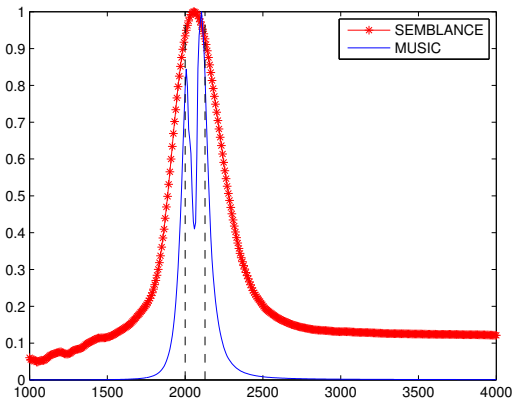

Figure 8: Parameter C determined using both MUSIC and semblance (point diffractor and a dipping reflector $\beta = 20^0$). The black dotted lines show the correct parameter locations.

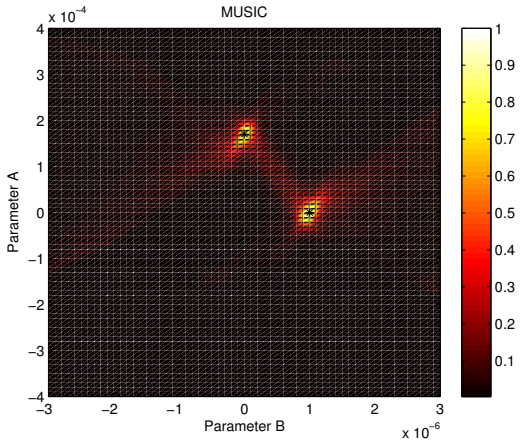

Figure 9: Determination of parameters A and B based on MUSIC for a diffractor and a dipping reflector $\beta = 20^0$. The black stars show the correct parameter locations.

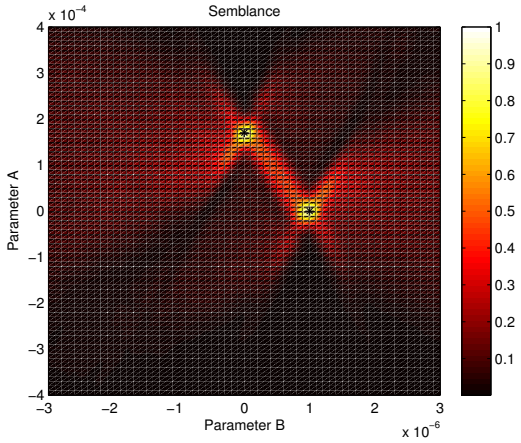

Figure 10: Determination of parameters A and B based on semblance for a diffractor and a dipping reflector $\beta = 20^0$. The black stars show the correct parameter locations.

Seismic MUSIC

To examine the performance of MUSIC compared to semblance in case of wideband correlated signals, we generated synthetic data based on the traveltime equations (16) for a CMP gather and equations (19) for a ZO section. The parameter search was performed within a time window of 25 time samples with the ZO traveltime being the middle sample and following a hyperbolic delay trajectory defined by the traveltimes. For the computation of the MUSIC pseudo-spectrum, the samples within the hyperbolic window were used to form the data covariance matrix and the associated eigen decomposition. In order to reduce the correlated source effect we performed spatial smoothing of the covariance matrix using 31 subarrays each consisting of 10 receivers for the CMP data and 37 subarrays each consisting of 15 receivers for the ZO data.

The results of the parameter search is shown in Figure 8 for the CMP data (i.e., determination of parameter C) and Figures 9 and 10 for the ZO section (i.e., determination of parameters A and B). It is obvious that both semblance and MUSIC can resolve parameters A and B, but MUSIC shows a higher resolution in general. However, for parameter C only MUSIC is able to resolve the two events.

CONCLUSIONS

In this paper we discussed the CRS traveltime parameters estimation problem in seismic signal processing. The conventiona1 semblance algorithm was found to generate a lower resolution estimates of the parameters. For the purpose of obtaining higher resolution parameter estimate, we replaced semblance with MUSIC algorithm. This algorithm allowed us to estimate the parameters within a resolution limit that is significantly better than the classical semblance. This work can be seen as a follow up of previous applications of MUSIC to single-parameter velocity analysis and slant stacks. Now, MUSIC is extended to Common-Reflection-Surface (CRS) multi-parameter estimation. Applications of the technique to first synthetic examples, consisting of dipping planar reflectors and point diffractors, and comparison to conventional semblance, confirm, at least for these initial situations, the expected far better resolution of MUSIC.

ACKNOWLEDGMENTS

E. Asgedom has been funded by a PhD-grant from the University of Oslo and the Norwegian Science Foundation. This work has been carried out while he was visiting State University of Campinas, Brazil. We acknowledge support of the present work by the *National Council of Scientific and Technological Development (CNPq)*, Brazil and the sponsors of the *Wave Inversion Technology (WIT) Consortium*.

REFERENCES

Biondi, B. and Kostov, C. (1989). High-resolution velocity spectra using eigenstructure methods. *Geophysics*, 54:832–842.

Du, W. and Kirlin, R. L. (1993). Discrimination power enhancement via high resolution velocity estimators. In *IEEE Acoustics, Speech, and Signal Processing*. IEEE.

Gelchinsky, B., Landa, E., and Shtivelman, V. (1985). Algorithms of phase and group correlation. *Geophysics*, 50(04):596–608.

Jäger, R., Mann, J., Hocht, G., and Hubral, P. (2001). Common-reflection-surface stack: image and attributes. *Geophysics*, 66:97–109.

Kirlin, R. L. (1992). The relationship between semblance and eigenstructure velocity estimators. *Geophysics*, 57:1027–1033.

Neidell, N. and Taner, M. (1971). Semblance and other coherency measures for multichannel data. *Geophysics*, 36:482–497.

Schmidt, R. O. (1986). Multiple emitter location and signal parameter estimation. *IEEE Trans. Antennas and Propagation*, AP-34:276–280.

Taner, T. and Koehler, F. (1969). Velocity spectra - digital computer derivation and applications of velocity functions. *Geophysics*, 34:859–881.

Zhang, Y., Bergler1, S., and Hubral1, P. (2001). Common-reflection-surface (crs) stack for common offset. *Geophysical Prospecting*, 49:709–718.

APPENDIX A: GENERAL HYPERBOLIC MOVEOUT

The CRS method uses the so-called generalized hyperbolic (normal) moveout, which is the natural generalization of the NMO, valid for CMP gathers, to CRS supergathers, in which source-receiver pairs are arbitrarily located around the (reference) central point, which is usual taken as a CMP. In 2D, the generalized hyperbolic moveoutdepend on three parameters, as opposed to conventional NMO, which depends on a single parameter (NMO-velocity).

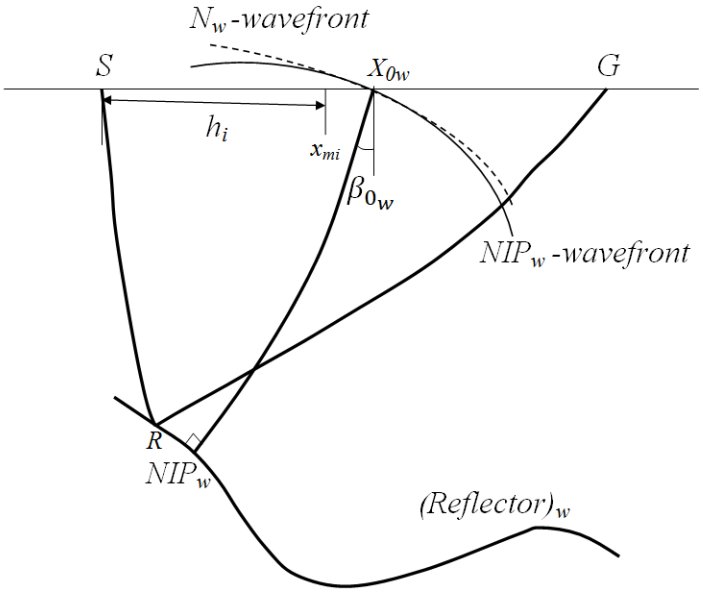

Figure 11: CRS parameters for a given source-receiver pair around a central ray at x_{0_w}.

Mathematically, the generalized hyperbolic moveout, $\tau_{i,\mathsf{w}}$, associated with the event, w, in the data, is specified by the zero-offset (ZO) traveltime, τ_{0_w}, and (reference) trace location, x_{0_w}, and given by (see Figure 11)

$$[\tau^{\theta}_{i,\mathsf{w}}(x_{m_i}, h_i)]^2 = [\tau_{0_\mathsf{w}} + A_\mathsf{w}(x_{m_i} - x_{0_\mathsf{w}})]^2 + B_\mathsf{w}(x_{m_i} - x_{0_\mathsf{w}})^2 + C_\mathsf{w} h_i^2 \,, \tag{A-1}$$

where x_{m_i} is the midpoint coordinate and h_i is the half-offset coordinate for the i-th receiver. Here,

$$\boldsymbol{\theta} = \{A_\mathsf{w}, B_\mathsf{w}, C_\mathsf{w}\} \,, \tag{A-2}$$

is the CRS parameter vector, with three parameters, A_w, B_w and C_w, to be estimated from the data. It is instructive to recall that these parameters are related to the angle and curvature quantities as follows (Jäger et al. (2001))

$$A_\mathsf{w} = \frac{\sin\beta_{0_\mathsf{w}}}{v_{0_\mathsf{w}}}, \quad B_\mathsf{w} = \frac{2\tau_{0_\mathsf{w}}\cos^2\beta_{0_\mathsf{w}}}{v_{0_\mathsf{w}}} K_{N_\mathsf{w}} \quad \text{and} \quad C_\mathsf{w} = \frac{2\tau_{0_\mathsf{w}}\cos^2\beta_{0_\mathsf{w}}}{v_{0_\mathsf{w}}} K_{NIP_\mathsf{w}} \,, \tag{A-3}$$

where K_{N_w} and K_{NIP_w} are the curvatures of respectively the normal (N) and normal-incident-point (NIP) wavefronts, β_{0_w} is the emergence angle and v_{0_w} is the medium velocity. All these quantities are evaluated at the central point, x_{0_w}. Still considering the CRS parameters, we make the following observations:

(a) In the CMP configuration of source-receiver pairs symmetrically located with respect to the central point, namely, $x_{m_i} = x_{0_{\mathsf{w}}}$, we have

$$[\tau^{\theta}_{i,\mathsf{w}}]^2(h_i) = \tau^2_{0_{\mathsf{w}}} + C_{\mathsf{w}} h_i^2 \,, \tag{A-4}$$

with the CMP, single parameter vector $\boldsymbol{\theta} = \{C_{\mathsf{w}}\}$. Moreover, we have the relation

$$C_{\mathsf{w}} = \frac{4}{v^2_{NMO}} \,, \tag{A-5}$$

with C_{w} given by the far most equation (A-3).

(b) In case the recorded data stems from a diffraction, the condition $B_{\mathsf{w}} = C_{\mathsf{w}}$ holds. This is because, as the reflector shrinks to a point, the N-wave turns out to be identical to the NIP-wave (Zhang et al., 2001). As a consequence, the hyperbolic moveout of diffraction (or *diffraction traveltime*), reduces to

$$[\tau^{\theta}_{i,\mathsf{w}}]^2(x_{m_i}, h_i) = [\tau_{0_{\mathsf{w}}} + A_{\mathsf{w}}(x_{m_i} - x_{0_{\mathsf{w}}})]^2 + B_{\mathsf{w}}[(x_{m_i} - x_{0_{\mathsf{w}}})^2 + h_i^2] \tag{A-6}$$

with the diffraction, two-parameter vector $\boldsymbol{\theta} = \{A_{\mathsf{w}}, B_{\mathsf{w}}\}$.